ERROR PROPAGATION FOR CLOSE-RANGE SINGLE IMAGE RELATIVE MEASUREMENTS

H. J. Theiss

National Geospatial-Intelligence Agency (NGA), 12310 Sunrise Valley Dr, Reston, VA, USA - henry.j.theiss.ctr@nga.mil

Commission V, WG V/1

KEY WORDS: Close range photogrammetry, Resection, Error propagation

ABSTRACT:

NGA uses the Compass software to perform relative measurements on images, usually taken at relatively close range from hand-held cameras. Compass currently does not have the capability to calculate a confidence interval around its computed relative measurements. This paper provides some results with both simulated and real data to illustrate how the matrix algebra associated with a photogrammetric resection can be used to also perform the rigorous error propagation required to derive a confidence interval around a distance measurement made on a single image. The approach is verified by comparing the actual errors in distance measurements to the confidence intervals around the estimates.

1. INTRODUCTION

The NGA's Image Chain Analysis (ICA) program uses collections of handheld imagery to derive three dimensional (3-D) Computer Aided Design (CAD) models of features such as aircraft. Currently, the ICA process does not incorporate error analysis. Therefore, the imagery derived CAD models have no means associated with it to aid in determination of the predicted error and reliability of their measurements. Beginning in Section 2, this paper describes a photogrammetric approach to incorporate error propagation into the ICA process. Section 3 then describes experimental results using simulated and real data. Finally, the paper ends with ideas for future work.

2. OVERVIEW OF APPROACH

The NGA's Sensor Geopositioning Centre (SGC) approach to performing error propagation for a single image is to mathematically model a resection. A resection is a procedure in photogrammetry that traditionally assumes that the image coordinates and associated ground coordinates of several points are measured, and adjustments to the camera position (XL, YL, ZL) and attitude (omega, phi, and kappa) are estimated in a least squares adjustment. These six elements are called the exterior orientation (EO) parameters. For this report, the camera's interior orientation (IO) is known from camera calibration; however, IO parameters such as focal length and principal point offset can be included in the resection if the geometry is sufficiently strong.

The typical NGA problem involves a close range image with no known absolute ground coordinates. However, it is often the case that several orthogonal linear features can be readily measured in the image. When appropriate, we constrain these linear features to be parallel to the X, Y, or Z axis of a local space rectangular (LSR) object coordinate system. Moreover, we need to specify the origin of the LSR system, preferably at an easily identifiable point in the image where three mutually orthogonal lines intersect. Finally, we need to know at least one distance in the object space in order for our derived camera position and any new distance measurements to be in known ground units, such as meters.

So, the SGC formulation requires a set of condition equations and constraint equations. The condition equations consist of the two collinearity equations per observed image point. These condition equations contain the six EO camera parameters (common for all points) and the three ground coordinates (X, Y, and Z for the specific point) as unknowns. The constraint equations consist of three types. The first type constrains the X, Y, and Z coordinates of the origin point to be 0, 0, and 0. The second type constrains each object line to be parallel to the X, Y, or Z axis. Such constraint requires two equations. For example, if the line is parallel to the Z axis (a vertical line), then the difference in X coordinates between the beginning and end of the line must be 0; and the difference in Y coordinates between the beginning and end of the line must be 0. The third type of constraint is a single equation to constrain the distance between two points to be equal to some measured value.

In order to calculate the confidence interval for a distance measurement on an image, we need to first compute the covariance matrix for the unknown ground coordinates that are estimated in the resection. Such covariance matrix is the inverse of the normal equations matrix; see [Mikhail et. al. and Mikhail] for details. Once the total ground covariance matrix has been computed, the parts corresponding to the endpoints of the "feature to be measured" are extracted. The covariance matrix for the relative vector between point 1 and point 2 is calculated as follows:

$$\Sigma_{rel} = \Sigma_{11} + \Sigma_{22} - \Sigma_{12} - \Sigma_{12}^{T} \quad (1)$$

Where Σ_{ij} is the 3 by 3 error covariance matrix for the object space vector between points i and j.

Σ_{rel} is the 3 by 3 error covariance matrix for the relative vector between points 1 and 2. If, for example, we know that such vector is parallel to the Z axis, then we are only interested in the (3,3) element of the matrix. The one sigma value for the uncertainty of the distance measurement would then be the square root of the variance; and the variance is the (3,3) element of the relative vector error covariance, Σ_{rel}.

3. EXPERIMENTAL RESULTS

This section consists of two subsections, one for simulated data and then subsequently real data.

3.1 Simulated Data

Figure 1 shows the linear features comprising the simulated data set. Note that some lines were intentionally made shorter than the others, so that the impact of length of known feature could be studied.

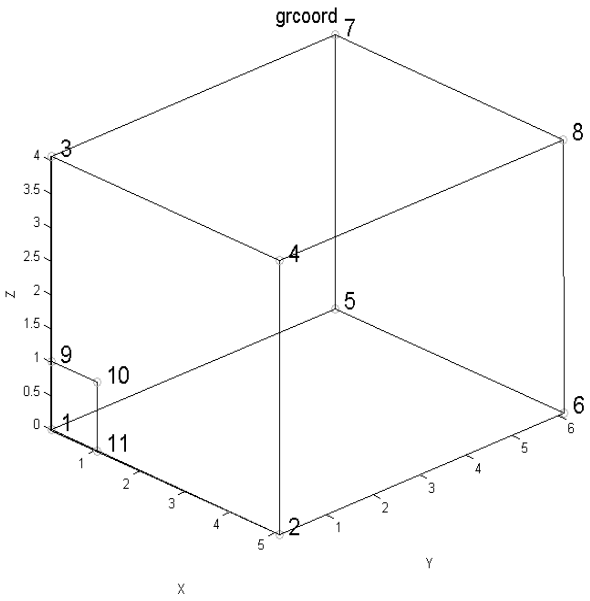

Figure 1: 3D plot of ground coordinates and lines comprising simulated data set.

Figure 2 shows the projection of the simulated linear features into the image space. Note that, due to perspective effects, parallel lines in object space project to lines that significantly deviate from being parallel in image space. An angular field-of-view of 60 degrees (horizontal direction of image format) was used in the simulation. As the field-of-view narrows, these object parallel lines would become more parallel in image space.

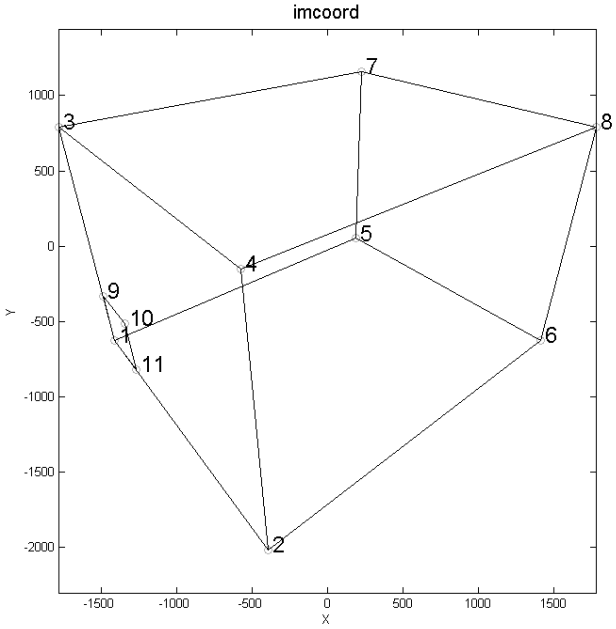

Figure 2: Image space view of points and lines comprising simulated data set.

Figure 3 shows the results from the simulated data, particularly how the measured errors compare to the confidence intervals. Note the high correlation between the measured and predicted errors. Also note how infrequently the errors exceed the 90% confidence interval. The predicted and measured errors become large for the cases when the relatively short vector is treated as the known distance.

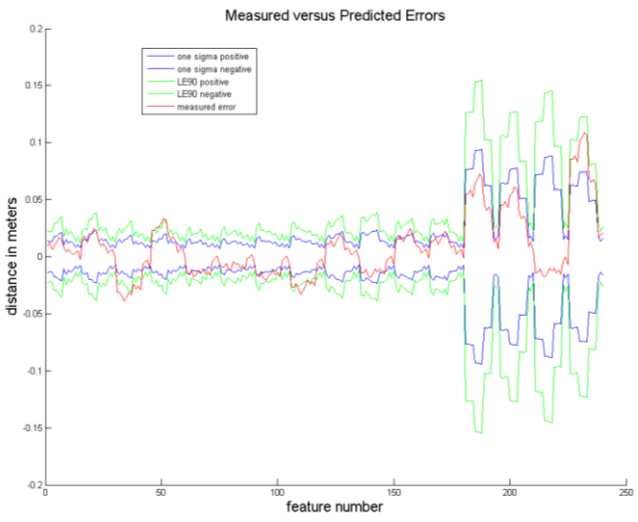

Figure 3: Measured versus predicted errors for simulated data.

Table 1 shows the results from the simulated data compared to truth, in terms of the mean, standard deviation, RMS, and confidence intervals (one-sigma and LE90). The results closely match the numbers expected by statistics; e.g. 68 percent should fall within one sigma.

Table 1: Simulated Data Error and Confidence Interval Results

Mean difference (meters)	Standard deviation (meters)	RMS (meters)	% below 1-sigma confidence interval	% below LE90 confidence interval
0.008	0.028	0.029	67	90

3.2 Real Data, Case 1

Figure 4 shows the results from the real data, particularly how the measured errors compare to the confidence intervals. Note again the high correlation between the measured and predicted errors. Also note how infrequently the errors exceed the 90% confidence interval.

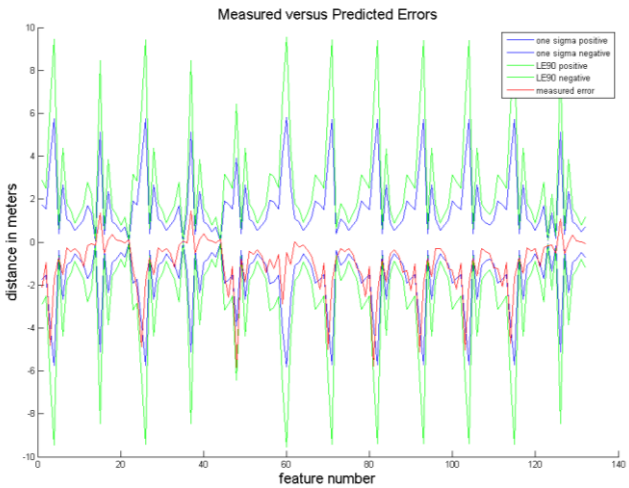

Figure 4: Measured versus predicted errors for Case 1.

Table 2 shows the results from the real data compared to truth, in terms of the mean, standard deviation, RMS, and confidence intervals (one-sigma and LE90). The results closely match the numbers expected by statistics; e.g. 68 percent should fall within one sigma and 90 percent should fall within the LE90 confidence region.

Table 2. Real Data (Case 1) Results

Mean difference (meters)	Standard deviation (meters)	RMS (meters)	% below 1-sigma confidence interval	% below LE90 confidence interval
-1.02	1.31	1.66	69	89

Although the error propagation appears to be working correctly, the magnitude of these predicted and measured errors are much larger than the authors expected them to be; i.e. on the order of one to two meters. The next real data case then investigates what additional constraints can be imposed in the math model in order to increase the precision.

3.3 Real Data, Case 2

In this new case, we imposed additional object space constraints to enforce that certain pairs of lines fell in the same vertical plane, thus resulting in 19 additional constraint equations. Also, the focal length was treated as an unknown in this experiment.

Figure 5 shows the results from the real data using these new constraints, particularly how the measured errors compare to the confidence intervals. As in Case 1, note the high correlation between the measured and predicted errors. Also note how infrequently the errors exceed the 90% confidence interval.

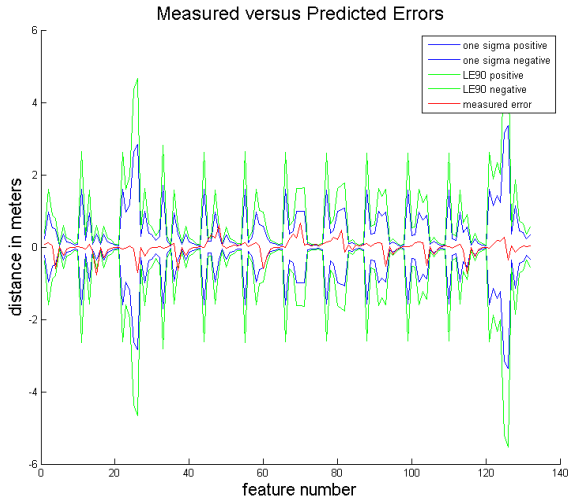

Figure 5: Measured versus predicted errors for Case 2.

Table 3 shows the results from the real data compared to truth, in terms of the mean, standard deviation, RMS, and confidence intervals (one-sigma and LE90). The results are a little conservative compared to those numbers expected by statistics; e.g. 68 percent should fall within one sigma and 90 percent should fall within the LE90 confidence region.

Table 3. Real Data (Case 2) Results

Mean difference (meters)	Standard deviation (meters)	RMS (meters)	% below 1-sigma confidence interval	% below LE90 confidence interval
-0.01	0.21	0.21	86	95

Figure 6 shows the measured and predicted errors as a function of the magnitude of the measured distance. A noticeable positive correlation exists, albeit not too great.

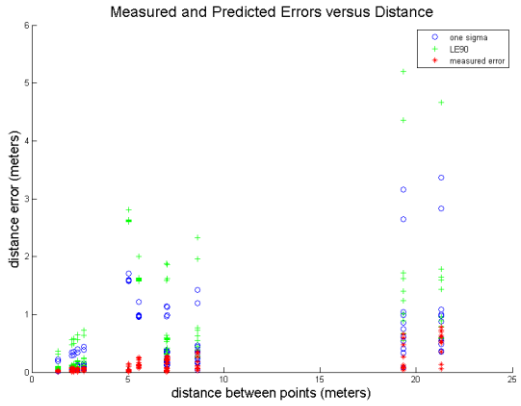

Figure 6: Measured and predicted errors versus distance.

Figure 7 shows the measured and predicted errors as a function of length of the control line used in establishing the camera model. A noticeable but subtle negative correlation exists.

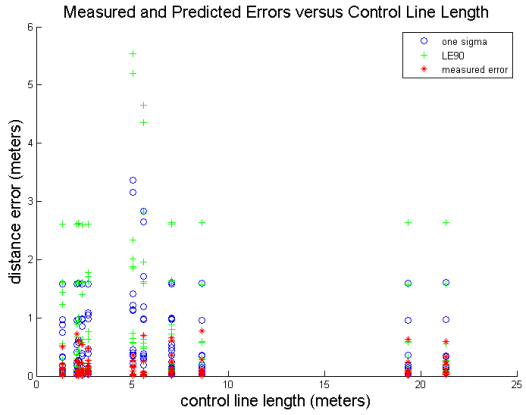

Figure 7: Measured and predicted errors versus control line length.

4. CONCLUSIONS AND FUTURE WORK

The SGC successfully developed a prototype that could perform rigorous error propagation for a single image, and therefore provide a confidence interval around any distance measurement. The measured errors are consistent with the predicted errors.

In the future, in addition to the investigation to improving precision (discussed in Section 3), the SGC plans to work on some of the following tasks:

- Compare error propagation performance between this paper's approach and classical close range formulations that use vanishing lines.
- Develop prototype for deriving confidence intervals around measurements other than distances.
- Develop prototype and/or provide recommendations for how to analyze the results and error propagation from the multi bundle analysis (MBA).
- Investigate impact of modelling lens distortion.

References from Books:

Mikhail, E.M., Bethel, J.S., McGlone, J.C., 2001. *Introduction to Modern Photogrammetry*. John Wiley and Sons, New York, NY.

Mikhail, E.M., 1976. *Observations and Least Squares*. University Press of America, New York, NY.

Acknowledgements:

The author acknowledges, with sincere thanks, the contributions from and open collaboration with scientists in the SGC as well as scientists and analysts in other divisions of NGA.